OPTIMIZED PROFILE EXTRACTION AND THREE DIMENSIONAL RECONSTRUCTION TECHNIQUE APPLIED TO BUBBLE SHAPES

A Thesis

by

GOKUL VASUDEVAMURTHY

Submitted to the Office of Graduate Studies of
Texas A&M University
in partial fulfillment of the requirements for the degree of

MASTER OF SCIENCE

December 2003

Major Subject: Nuclear Engineering

OPTIMIZED PROFILE EXTRACTION AND THREE DIMENSIONAL RECONSTRUCTION TECHNIQUE APPLIED TO BUBBLE SHAPES

A Thesis

by

GOKUL VASUDEVAMURTHY

Submitted to Texas A&M University
in partial fulfillment of the requirements
for the degree of

MASTER OF SCIENCE

Approved as to style and content by:

Yassin A. Hassan (Chair of Committee)	Gerald L. Morrison (Member)
William H. Marlow (Member)	William Burchill (Head of Department)

December 2003

Major Subject: Nuclear Engineering

ABSTRACT

Optimized Profile Extraction and Three Dimensional Reconstruction Technique Applied to Bubble Shapes.

(December 2003)

Gokul Vasudevamurthy, B.E., Bangalore University

Chair of Advisory Committee: Dr. Yassin A. Hassan

In order to predict the behavior of bubbly flows, it is necessary to know the three dimensional profiles of the bubbles present in the flow. With advancements in the field of flow visualization, accurate reconstruction of the bubble shape has become necessary. The PIV and the SIV techniques, used to acquire images of particles and bubbles, have been found to be extremely useful in this regard. The study, development, implementation, applications and limitations of a unique reconstruction technique applied to various regular and irregular bubble shapes, using the two orthogonal projections of the three-dimensional bubble profiles as captured by the SIV cameras are presented here. The technique is a blend of neural networks, combinatorial optimization and advanced computer aided design methods. The technique involves the robustness and ruggedness of the neural network approach and the flexibility and reliability of advanced computer aided design methods. The technique uses a well-known problem in neural networks and combinatorial optimization known as the Traveling Salesman Problem approach to identify the bubble boundaries on the images. An optimization solution technique known as the Simulated Annealing technique is employed to solve the Traveling Salesman

Problem and obtain the bubble profiles. These results are employed to reconstruct bubble shapes using NURBS computer aided design software.

Two main applications of this technique are demonstrated and the results are found to be promising. The first application included the calculation of the void fraction at a particular depth of the channel/ pipe and at a particular radius of the channel. The second application was Lagrangian tracking of bubbles, wherein the centroids of the bubbles were tracked between image frames to determine the linear and transverse velocities of the bubbles.

This technique has shown scope for development including the development as integrated bubble surface reconstruction software and advanced modifications at various levels for efficient and accurate reconstruction.

ACKNOWLEDGEMENTS

I would like to express my gratitude to my graduate advisor, Dr. Yassin A. Hassan, who gave me an opportunity, the freedom and support needed to implement this particular research idea and make it a fruitful endeavor. Dr.Hassan deserves my special respects for having introduced me to the field of Particle Image velocimetry which is emerging fast as the visualization tool of the future. His valuable advice and suggestions will always be cherished.

I would like to thank Dr. Gerald Morrison and Dr. William H. Marlow for agreeing to serve on my thesis committee and for the invaluable support that they have extended during my association with them.

A special mention is required of Dr. Bruce McCormick of the Department of Computer Science, TAMU, for his kind guidance in the field of Neural Networks and Pattern Recognition, which was the key for making this research a success.

I would like to express my sincere thanks to Dr. Javier Ortiz Villafuerte and other colleagues of the two phase flow lab for having extracted invaluable data without which this research would have not been practical.

I would like to thank Dr. Sridhar Hari and all my friends in the department of Nuclear Engineering for the technical and moral support they gave me throughout.

Finally, I would like to thank Dr. William Burchill and all the Professors of the Department of Nuclear Engineering , TAMU, for their support.

TABLE OF CONTENTS

Page

CHAPTER Page

LIST OF FIGURES

Page

Page

LIST OF TABLES

Page

NOMENCLATURE

PIV : Particle Image Velocimetry

PSIV/SIV : Pulsed Shadow Image Velocimetry

TSP: Traveling Salesman Problem

SOM: Self Organizing Maps

SA : Simulated Annealing

CHAPTER I

INTRODUCTION

Bubbly flow forms an important flow regime in two phase flows. They have been well studied and many correlations have been established. Different techniques have been devised to estimate the important parameters of such flows like the void fraction for example. Presence of bubbles in the flow influence the behavior of the flow as a whole and the method the flow is analyzed. The very fact that bubbles influence the velocity local to their surfaces make things complicated. Presence of bubbles change the velocity, the void fraction and heat transfer parameters. As bubbles form a part of the flow, bubble centroid velocities have to be estimated. Owing to the importance of study of bubble dynamics and behavior, there is an imperative need to keep track of the bubbles. Parameters like the interfacial velocity, bubble centroid velocities and the void fraction are important and needed to determine the hydrodynamic and heat transfer mechanisms between two phases.

Recently various tools have been developed and tested to study bubbly flows. PIV and PST are the most prominent among the techniques used for flow visualization [1, 2, 3, 4, 5]. These tools are preferred to hot wire anemometry and Laser Doppler techniques specifically due to their non-intrusive nature and full field velocity measurements respectively. These analysis techniques are currently regarded as the best-suited flow visualization techniques.

This thesis follows the style of *Journal of Nuclear Technology*.

The PIV technique uses a single camera to acquire images, which contain particles and bubbles. Hence only the planer view of the flow is obtained. However, to determine the void fraction, calculation of the surface area, and hence the reconstruction of the actual shape of the bubbles at a particular depth of the channel/ pipe is required. Limitations on the part of the camera systems, which provide only one-dimensional profile of a bubble, makes it difficult to estimate complex parameters, like the surface area of the bubble from two-dimensional view.

A new technique called the pulsed shadow image velocimetry (PSIV / SIV) evolved to augment the study of bubble behavior and the three dimensional surface visualization. In this technique, 'shadows' of bubbles in the flow are captured by two or more cameras. The procedure of image acquisition and systems is described in detail by Javier (2000)[4] and Donald Todd (2002)[5]. The study of various reconstruction techniques was found necessary to calculate the parameters of bubbles in a flow. Especially with the advancement of three-dimensional PIV techniques, reconstruction of the bubble shapes in three dimensions has become an acute necessity. Also reconstruction of bubble shapes would help us understand the mechanisms of wakes, interfacial velocities and other parameters which help in estimating the local void fraction and the bulk void fraction. These are found to be of importance in heat transfer calculations.

It is now common to employ neural networks for flow measurements and flow behavior predictions, especially for flow visualization. Cenedese, Romano, Paglialunga & Terlizz (1992)[6], Gilles (1998)[7] and Hassan & Philip (1997)[8] give elaborate description of such methods. The technique presented here dwells on the use of neural network

approach to reconstruct the actual three-dimensional profiles of the bubbles in a flow using two orthogonal one-dimensional bubble profiles. This technique was developed and tested on various irregular bubble shapes. The technique was developed in stages with a goal of extracting the two dimensional bubble profiles using a well-known classical combinatorial optimization problem called the 'Traveling Salesman Problem' (TSP) [9, 10, 11]. The TSP was solved using an optimization technique called the 'Simulated Annealing Technique' (SA) [12, 13, 14]. NURBS [15, 16] based CAD was employed (Non-Liner Rational B- Splines) for three dimensional reconstructions. Alternative Solutions to the TSP, as like the Kohonen self-organizing map [17, 18, 19] and the elastic net[9] were also tested.

The feasibility of developing an integrated design environment to achieve the bubble reconstruction using high level programming and computer aided design is studied. Studies were made on the feasibility and compatibility of different available software used in three dimensional reconstruction and high level programming. After a detailed analysis, MATLAB and RHINO CAD[20] (Rhino 3.0) based on the NURBS methodology were selected to solve the TSP-SA and NURBS three-dimensional Reconstruction. A free evaluation copy of the RHINO CAD was used to demonstrate the capability of the technique. Advanced features of the NURBS RHINO CAD's– surface modeling tools like the rail revolve, match, and other advanced commands were studied and were applied suitably for the technique.

The technique is extended to analyze and reconstruct bubble shapes in batches. Each batch consists of a large number of bubbles (>10) selected from the shadow images.

Two applications of the technique to estimate of the void fraction at a given depth and bubble trajectory tracking are demonstrated.

CHAPTER II

BACKGROUND FOR THE PRESENT WORK

This section focuses on understanding the need for the development of a unique reconstruction technique with brief discussions on different methods used for this purpose in the past with a general reference to methods of Particle Image Velocimetry (PIV), Particle Tracking Velocimetry (PTV) and Pulsed Shadow Image Velocimetry (SIV).

Overview of the PIV, PTV and PSIV Techniques

In PIV technique, traces of micro-particles known as 'seeds' are added to the flow and a powerful laser light is used to illuminate a thin cross-sectional plane of the channel/pipe. A high-resolution image acquisition system consisting of a digital camera and computer hardware, acquire and store the images for further analysis. These are found to be extremely reliable for single phase flow analysis. The images are acquired in a known sequence and a known interval of time. Assuming that the particle does not move out of the light sheet, the distance traveled by the particle is calculated by analyzing two consecutive images. The time interval between the laser shots is known; hence the magnitude of the instantaneous velocity can be calculated. Recent publications [21, 22, 23] indicate that PIV can be successfully and efficiently employed in the analysis of certain two phase flows provided that both phases can be distinguished.

A simple, PIV technique is not inherently built to analyze two phase flows. For example in analyzing a bubbly flow, it does not take into account the bubble velocities as it treats all flows like single phase flows. The bubbles appear as big 'Blobs' on the images. In the PIV analysis, the big blobs are just unwanted areas present in the data, which will be ignored or removed before analysis of the images. A PIV technique, which basically employs the cross correlation method, will not be able to find any correlation in these areas due to absence of particle or seeds. However these techniques generally incorporate the interpolation mechanism and hence tend to substitute interpolated velocity vectors in these areas where no correlation is found. If one compares the result of PIV analysis of bubbly flow and a single-phase flow it would be quite unsurprising if no difference is found. Some recent publications indicate the necessity to include the bubble velocities and the importance of bubble mechanics [4, 5, 24, 25, 26].

The PIV images contain indistinct bubbles. Not enough information is available about the three-dimensional profile of the bubbles in the PIV images. Hence an alternate set up called the 'Pulsed Shadow Image Velocimetry' is employed [4, 5, 27, 28]. Detailed explanations of the set up are discussed in Donald Todd (2001)[5]. Two 'shadow' cameras acquire views in the two orthogonal planes. These views can be named as front and side for convenience. Care has to be taken to see that the resolutions of both the cameras are properly adjusted and the data acquisition system is properly synchronized.

In contrast to the PIV, the PTV technique [3, 29, 30, 31] which is considered on par with the PIV, does not use any interpolation schemes. It is built to track each and every individual particle. Hence the number of velocity vectors obtained is sometimes lower

and non-uniformly distributed. However this feature makes it more accurate. The biggest advantage about PTV technique is the scope for inclusion of the bubble velocities if they could some how be estimated and superimposed on the flow velocity profile. For this the bubble shapes have to be reconstructed and their velocities have to be estimated.

Overview of Bubbly Flow Investigations

More recently, PIV has been extended to investigate bubbly flows [4, 5, 32]. When the flow regime turns bubbly, it becomes necessary to account for the behavior of the bubbles. The bubbles move with a different velocity compared to that of the particles/seeds (hence the flow) and therefore influence the overall system velocity. They also influence the velocities, behavior and shapes of other bubbles in the flow. The bubble motions become more chaotic as the flow velocity increases and are not governed by any hardbound rule. Though attempts have been made to predict the behavior of bubbles and to study their dynamics, the conclusion that one agrees upon is that the bubble shape and behavior increase in complexity as the velocity and the number density of the bubbles in the flow increase.

Overview of Different Bubble Reconstruction Methods

In a real scenario it is often observed that the bubbles in the flow are highly chaotic in shape and behavior. Bubble–wall and bubble-bubble interactions and the flow regime characteristics ensure that the bubble shapes are not exactly ellipsoidal and their

surfaces are not smooth at all instants of time, as they are often assumed. Collisions may tear off the bubbles or seriously distort their shapes.

More recently, researchers have indicted that bubble shapes can be described by non- dimensional parameters like the bubble Reynolds number, the Morton, the Eotvos and the Weber numbers [5, 28, 29]. They have also indicated that the bubble behavior changes in case any of these parameters are considerably altered. Renewed efforts have been made to reconstruct the bubble shapes [4, 5, 15] using various available techniques. One such simple methodology assumes bubbles as simple Ellipsoids or Spheres. Turner, Anderson, Mason & Cox (1999)[33] describe a method of fitting an ellipsoid to a given three dimensional data. Forbes (1990)[34] describes robust techniques to fit a sphere to the available data. Javier (1999)[4] and Donald Todd (2001)[5] propose similar techniques and discuss the advantages and disadvantages of assuming that the bubbles are either spherical or ellipsoidal. In real scenario it is very hard to establish equivalency between the original shape of the bubbles and the assumed spherical and ellipsoidal shapes. This brings forth ambiguity in determining the volume and the centroid of the bubbles. This problem is augmented by the absence of a robust technique to establish accurate equivalency of the shapes.

Zhang & Pang (2000)[15] demonstrate the applicability of NURBS modeling to reconstruct bubble shapes. A detailed study was made in the paper named 'NURBS Blobs for Flow Visualization'. The NURBS technique appears to be in close association with the one that is presented here. The difference between the presented technique and the existing technique is that the bubble has to be reconstructed with two available

orthogonal views if one could somehow extract their profiles from the images as simply connected contours.

Absence of an accurate and robust three dimensional shape reconstruction technique and the problems associated with establishing shape equivalency with assumed bubbles shapes have set the stage for the development of this unique technique.

CHAPTER III

DEVELOPMENTAL STAGES OF THE TECHNIQUE

This section discusses in brief the significant 'stages' of the technique. The technique was developed in stages, facilitating the setting up of an integrated procedure which could be used in the future to develop relevant software. A detailed account of each step and associated results are presented in the following sections. The flow diagram of the technique is shown in Fig.1.

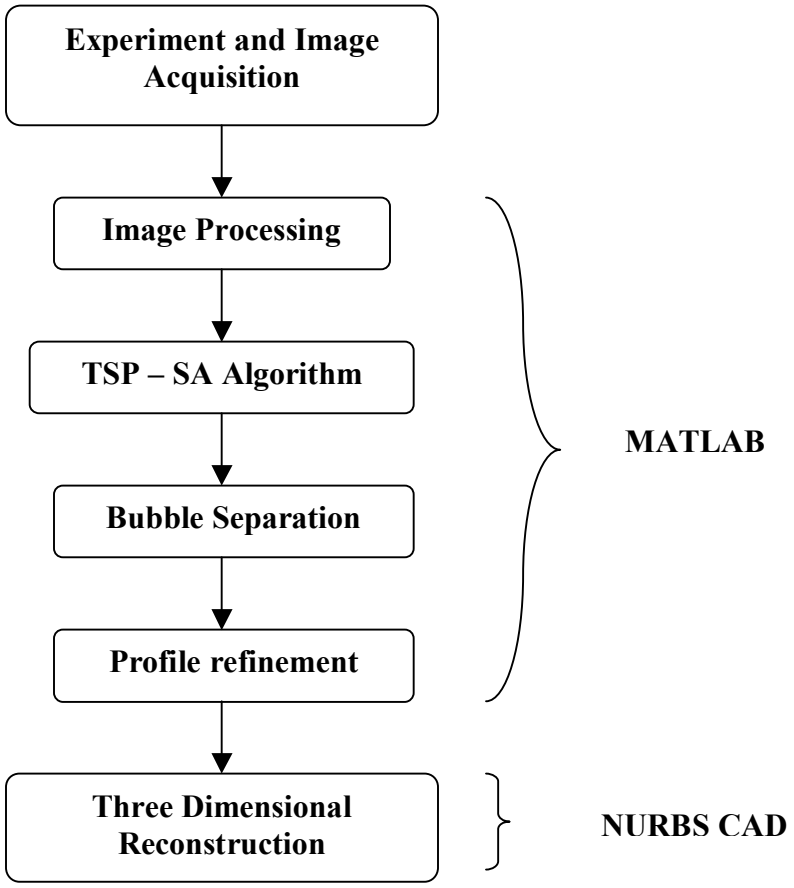

Fig.1. Logical Flow Diagram of the Technique

Image Acquisition and Experiment

This stage consists of the experimental set up and data acquisition. The data is in the form of shadow images. The data images are named sequentially in pairs. A detailed account of the setup and nomenclature can be found in Javier (1999)[4] and Donald Todd (2001)[5].

Image Processing

This basically includes threshold and refinement of the image. The pixel 'yield' using different established software was tested. A code in MATLAB was also developed based on the histogram transformation method with the idea of integrating the whole scheme into a single program. Three unique and different threshold schemes were developed and tested.

Traveling Salesman Algorithm and Solution Technique

The feasibility of applying the Traveling Salesman technique was studied to extract the bubble profiles from two orthogonal planar views as obtained from the shadow images. The TSP is found to give a closed contour of the route that is taken by a salesman traveling among pre-designated co-ordinates (on a map) called cites. An analogy was observed between the points on edges of the threshold image of the bubbles and the cities on the tour contour of the TSP. This analogy paved the way for the use of TSP to extract the bubble profiles from the two planar views. The most important part of

the TSP is the solution. The self-organizing maps approach discussed by Kohonen (1982b, 1991, 1982a) [17, 18, 19] was tested and a neural net was built to test this method. Another powerful method known as the Simulated Annealing technique [12] was tested to solve the TSP.

Bubble Separation Technique

This was found to be one of the most difficult steps of the technique is the bubble separation step. Though bubbles may be physically separate, the planar view they appear to overlap, making it impossible to know their complete contour profile. Two simple methods were developed, tested and successfully employed to overcome this limitation. They are discussed in detail in the following chapters.

Profile Refinement

Due to the image resolution limitations and the histogram threshold technique used to obtain the bubble profiles, the contours obtained are observed to be highly rough and discontinuous. This roughness or discontinuity of the bubble profile has to be corrected. A scheme was adopted to deal with this limitation.

Three Dimensional Reconstruction

The last step of the technique was three-dimensional reconstruction employing the CAD software. A NURBS based CAD Software was used. NURBS is an accepted standard for industrial designs. Surfaces and curves are constructed using various control

points. An assumed analogy between the control points of NURBS and the TSP co-ordinates (Points on the bubble profile) shows the feasibility of this whole technique. Extensive interface programs were developed to link the high level data analysis tool (MATLAB) with the CAD software. A free evaluation copy of the RHINO CAD[16] was employed to do the reconstruction. Various tools like the Rail revolve, Match surfaces, Rotate, Rotate-3D and various commands available in Rhino – 3.0[16] were found handy in the reconstruction. The step also involved matching of centroids of profiles in the two views and bubble placement. Based on the type of application that employs this technique, various options like section at a particular depth, the projection of a section on a plane to estimate the area of the bubble at that depth and estimating the centroid of the three dimensional profile were also found useful.

CHAPTER IV

EXPERIMENTAL SET UP AND DATA ACQUISITION SYSTEM

This chapter briefly discusses the experimental setup and the data acquisition systems developed in the laboratory to investigate bubbly flow in vertically oriented cylindrical section of a pipe. The test data for the technique was derived from experiments previously conducted by Javier (1999)[4] and Donald Todd (2001)[5] at the Texas A&M Multi-phase flow laboratory. Description of the details of experiment conducted and the methods used to record sequential data can be found in Donald Todd (2001)[5] and Javier Ortiz (1999)[4].

Overview of the Experimental Setup

A fully operational experimental facility capable of operating in single phase, bubbly, slug and annular flow regimes was used to acquire data in the form of consecutive images. The facility can operate efficiently in single phase and bubbly flow regimes with the liquid Reynolds number ranging from 0 to 20335. Two different types of visualization methods have been combined to form a single data acquisition system. The PIV technique is used to measure parameters for the continuous liquid phase and the SIV technique is employed to probe the bubbles. The experimental setup and the measuring instruments are well calibrated before the conduction of the experiment. Donald Todd (2002)[5] and Javier (1999)[4] discuss the experimental facility and calibration in detail.

The experimental facility consists of two pumps, two reservoir tanks, many flow meters, hoses, a cylindrical pipe made of Pyrex and a bubble generator. The two pumps are used to control the bubble distribution. The secondary pump provides the needed liquid mass flow. The bubble generator generates air bubbles utilizing the shearing action of the secondary flow with injected air, which is perpendicular to the secondary flow. The details of the air-water experimental setup are described in Donald Todd (2002)[5] and Javier Ortiz (1999)[4]. A sketch of the air-water experimental facility is shown in Fig.2.

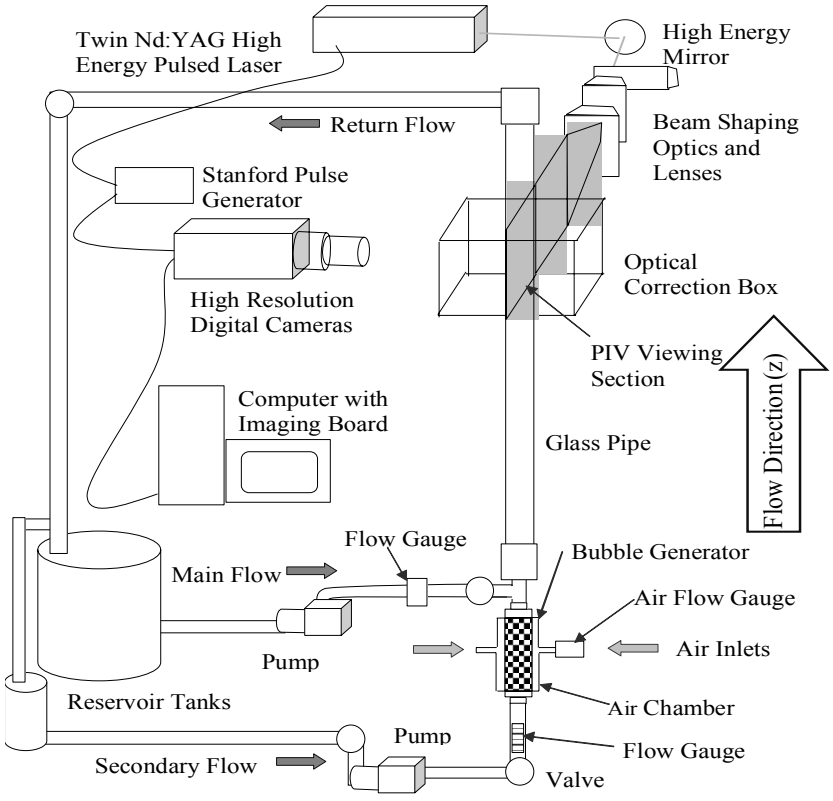

Fig.2. Air-Water Experimental Facility

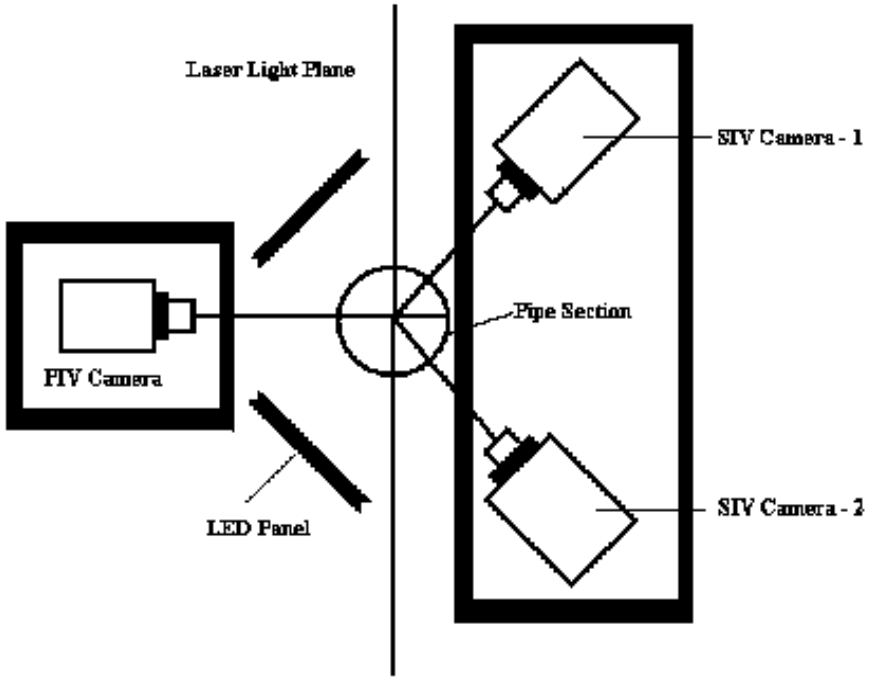

Fig.3. Schematic of the Experimental Setup for PIV /SIV

Fig.3 shows the schematic of the experimental setup for PIV/SIV. The Laser light from a YAG laser illuminates the PIV camera. Details of the laser used and the timing diagrams can be found in Donald Todd (2001)[5] and Javier Ortiz (1999)[4]. The two SIV cameras are placed at right angles to each other. The angle between the horizontal axes of the PIV and SIV cameras is 120 degrees. Two light emitting diode panels provide the illumination for the SIV cameras. In the system used, the SIV cameras shot the images simultaneously, obtaining the front and the side views of the bubbles. The Experimental set up, image acquisition, calibration and solution for the resolution limitations have been presented in detail by Donald Todd (2001)[5]. Procedures for recognizing a given bubble in

the two views have also been presented in detail. Fig.4 and Fig.5 show typical PIV and SIV images respectively acquired by the systems and used for analysis. Fig.6 shows the two orthogonal shadow image views. These are named as front and side views for three dimensional reconstructions.

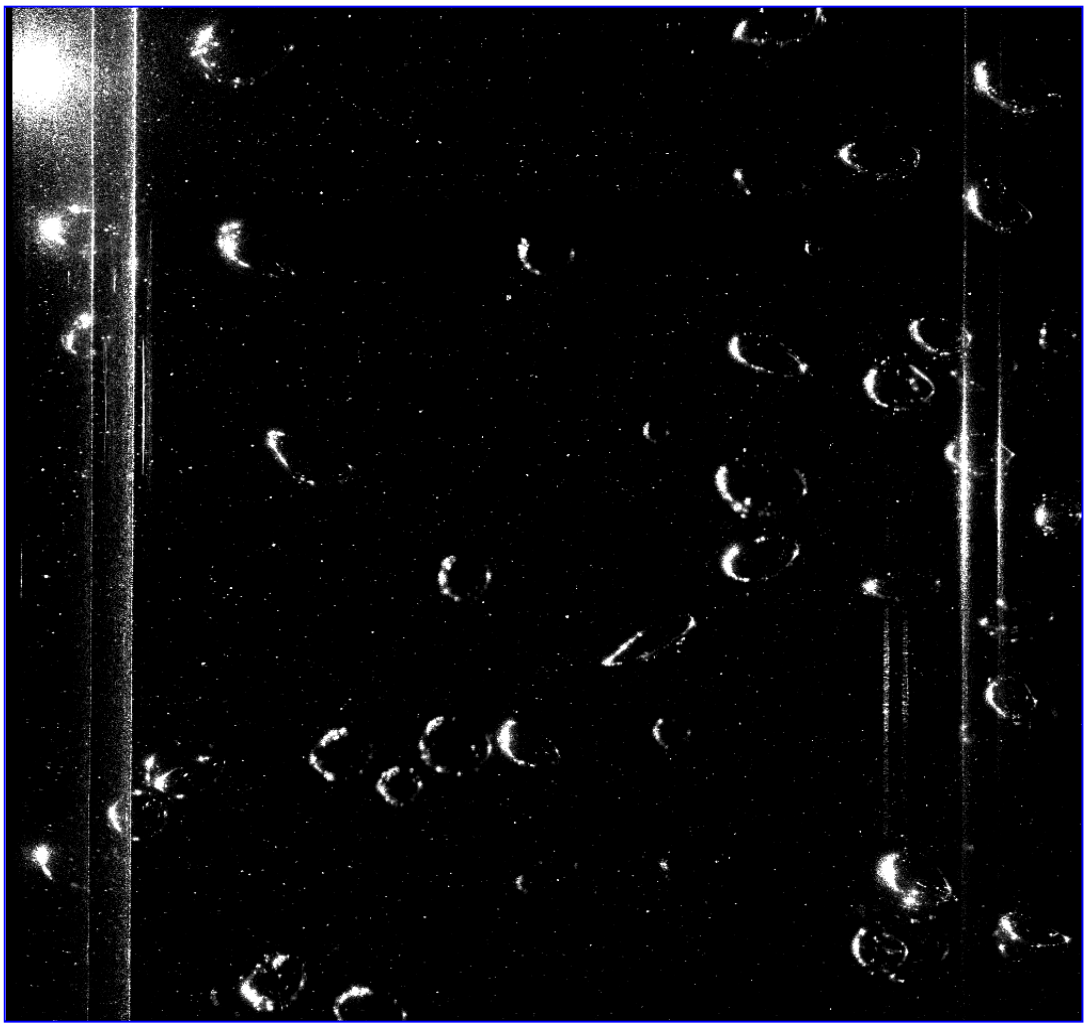

Fig.4. A Typical PIV Image

Fig.5. A Typical SIV Image

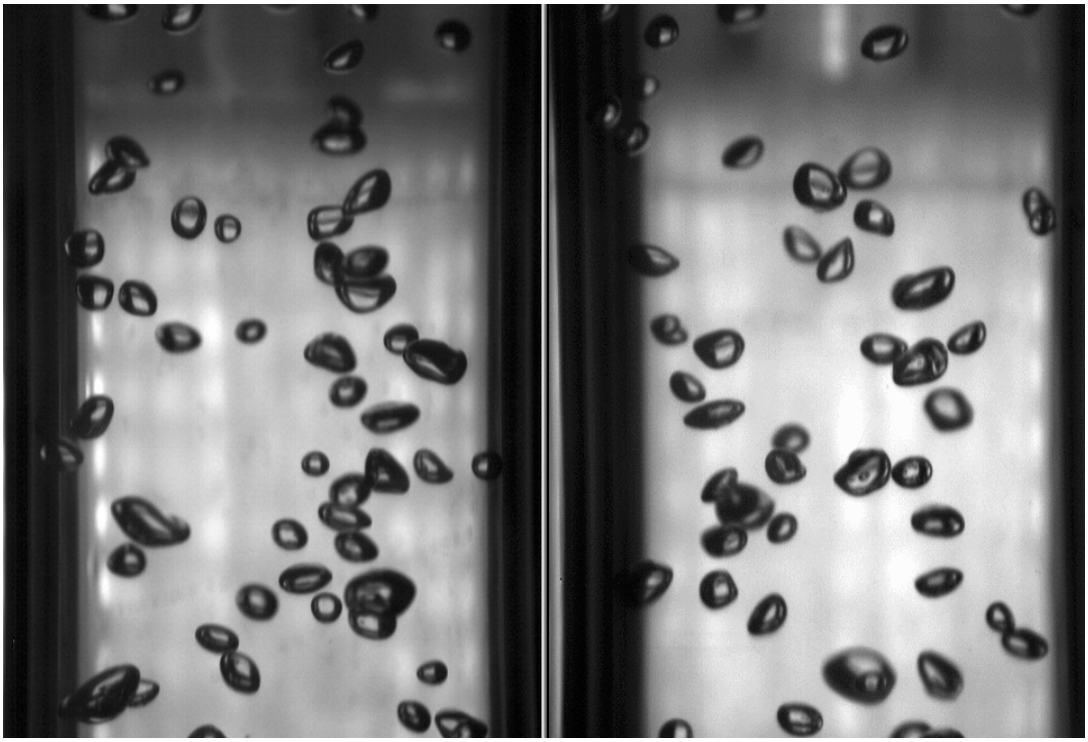

a. Front View b. Side View

Fig.6. Two Orthogonal Shadow Image Views

CHAPTER V

IMAGE PROCESSING

This chapter discusses the second stage of the technique wherein the raw images from the SIV data acquisition systems are processed in several sub stages so that the images can be cleaned and converted to binary images which can be used directly in profile extraction.

Overview of the Image Processing Stage

The SIV images obtained are crude and hence need some processing before analysis. Upon careful observation of the SIV images, the bubble boundary appears to be distorted. This is an effect of reflection on the bubble surface. As a result optical noise becomes prominent at such spots on the images where reflection is predominant, limiting accurate detection of the exact boundary of the bubbles. This noise has to be accounted. For small bubbles these can be ignored. But normally this can be avoided by using filters in the experimental stages and during thresholding in the image analysis. In the present technique, a thresholding scheme was developed and employed to minimize the loss of data due to the effects of reflection. Though this scheme was found to induce some amount of uncertainty, it appeared to be suited best for the available data. The scheme was divided into parts. First, the shadow images were inverted to obtain the 'digital negative' of the original image. This step helps to determine the exact number of bubbles in an image visually.

Thresholding

The next step after visual recognition is to threshold the original gray scale image. Many available, image processing software like Lab view and MATLAB were used to obtain different threshold limits and a brief comparison were made. The need to integrate this step into the technique, led to the development of a simple code based on the histogram transformation technique [35, 36, 37] in MATLAB to threshold the digital images. Intensity of the pixels was taken as the measure of the image quality to determine the threshold. Due to the uneven placement of bubbles in the plane of illumination, each and every bubble will have a different distribution of pixels intensities [38]. Lack of standardization of threshold and uniform intensity distribution on the bubble surface, makes it necessary to threshold the bubbles on an individual basis. However owing to overlaps and difficulty in separation and extraction of the profiles, at this stage, there was a need to develop a unique standard procedure to determine the threshold limit that would be applicable to the entire image, choosing all the pixels that lay between the two limits The limits[35] were chosen based on the 'yield' in the number of co-ordinate points on the bubble boundary. This also indicates the number of cities that has to be input to the TSP-SA algorithm. The wide range in pixel intensity distributions, required determination of the average pixel yield such that the threshold limit that returned the maximum yield and hence could be applied to all bubbles in the image. The average was calculated using three methods resulting in three grades of thresholds.

The Grade 'A' Scheme

The average yield was calculated using one third the number of bubbles in an image. One third of the bubbles were selected at random from the image and the average yield was calculated. Though the expected yield was found to be less in this scheme, it was found to be the simplest and least time consuming method for reconstructing large number of bubbles. Fig.7 shows Grade A scheme applied to a shadow image.

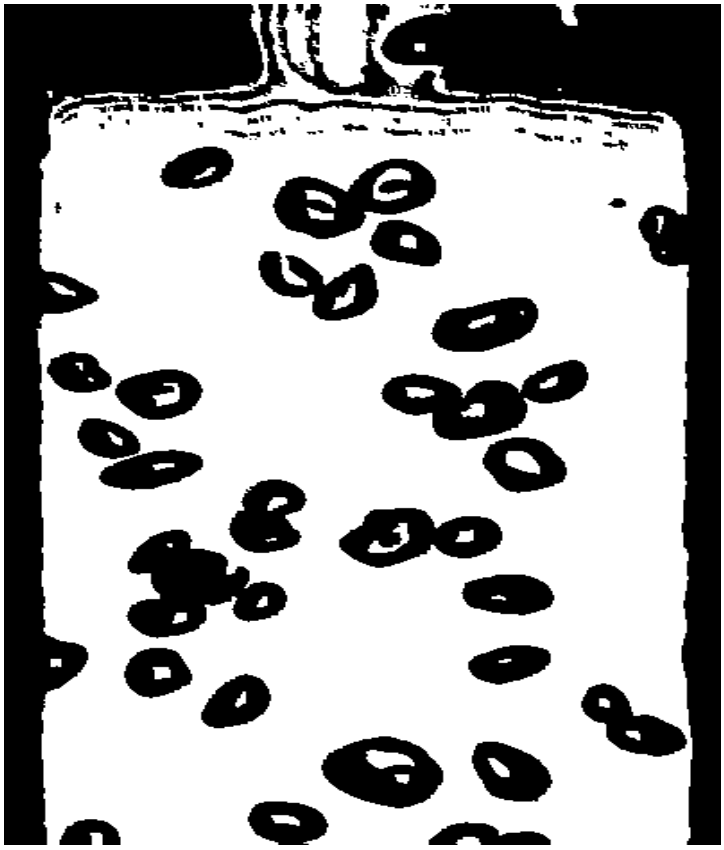

Fig.7. Typical Grade A Threshold Applied to a Shadow Image

The Grade 'B' Scheme

In this method, the average yield was calculated using more than half the number of bubbles. The numbers of bubbles selected for averaging from the center of the image were equal to the number of bubbles selected from away from the center of the image. This method struck a balance between the bubbles with high intensities and low intensities, which was not considered in Grade A. In addition to the yield being high, this was found to be the most effective and moderately fast method where the number of bubbles involved was high. Fig.8 shows Grade B thresholding. The only disadvantage of this method was that it had a poor resolution of bubbles close to the wall and in regions where the wall reflections were considerable.

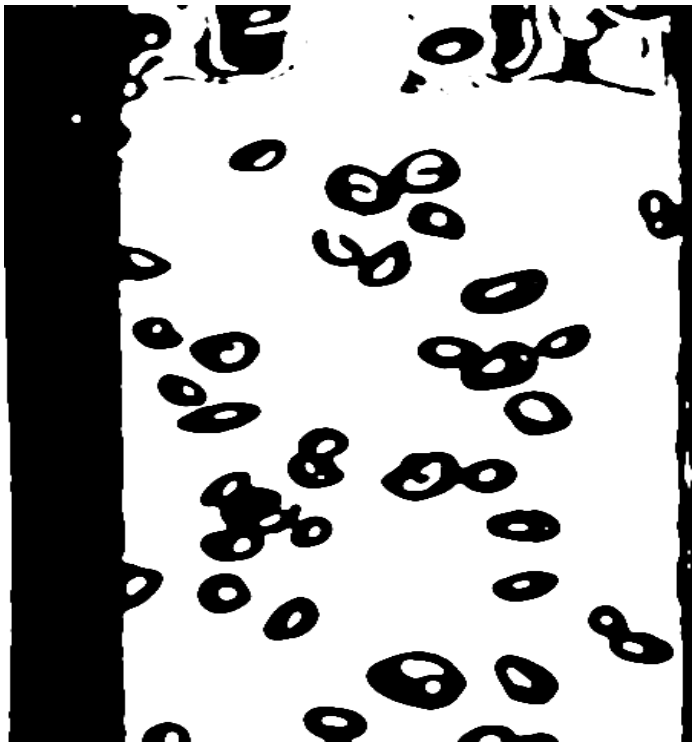

Fig.8. Typical Grade B Threshold Applied to a Shadow Image

The Grade 'C' Scheme

In this method the average yield was calculated taking all the bubbles in the image into consideration. Individual bubbles were selected and thresholded. The pixel yield in individual case was calculated. The average yield was calculated using these individual yields and the number of bubbles in the image. This method was effective and reliable with images containing lesser number of bubbles and with images where all the bubbles were in the center of the image rather towards the periphery. This method failed in cases where bubbles in the images were close to the wall. The failure is due prominent multiply reflections on bubble surfaces and the reflections at the channel wall itself. A gray scale intensity limit of 70 to 255 on a scale 0 to 256 range was chosen and found to be most satisfactory. A sample original and threshold bubble images form a stagnant flow is shown in Fig.9 and Fig.10.

Fig.9. Isolated Bubble Shadow Image

Fig.10. Grade C Threshold Image

Conclusion

It is clear from the methods described above that a single method can be used to obtain the thresholded profiles of all the bubbles in a particular image. Hence a combination of the Grade B and Grade C methods were used to obtain bubble image thresholds. Table.1 shows the average yield in case of Grade A, Grade B and Grade C threshold methods.

Table.1. Pixel Yield with Different Threshold Schemes

Grade A (Range of average boundary pixel Yield per bubble considering 10 images)	Grade B (Range of average boundary pixel Yield per bubble considering 10 images)	Grade C (Range of average boundary pixel Yield per bubble considering 10 images)
45 to 100 (Pixels / Cities)	78 – 290 (Pixels / Cities)	258 to 342 (Pixels / Cities)

CHAPTER VI

THE TRAVELING SALESMAN PROBLEM AND SOLUTION

This chapter discusses the Traveling salesman problem, the analogy between a bubble boundary profile and the path taken by the salesman covering all the cities and the techniques used to solve the TSP. The solution to the TSP is as important as the problem itself. Without a proper solution, the TSP is of no use. Various methods have been developed time and again to solve the TSP efficiently. Most popular among them are the SOM and the SA techniques. This chapter depicts in brief the two methods, their algorithms and compares their performances.

The Traveling Salesman Problem

The Traveling Salesman Problem (TSP) is a well known problem in the field of combinatorial optimization [9, 10]. The problem deals with finding an optimum path of travel, taken by a salesman to travel among pre-located cities. The cities are characterized using the co-ordinates on a map. The constraint on the solution is that the salesman should not visit the same city twice except the city he starts form. Hence the solution is a closed path or a contour.

The Analogy

Careful observation suggests that an analogy exists between the coordinates of the points on the bubble boundaries and the cities associated with the TSP. Utilizing the

advantage of this analogy, the TSP was extended to extract the bubble profiles in the SIV images. The point co-ordinates on the thresholded bubble images can be simply connected to find a closed contour to get the extrapolated boundary of the bubble and a very good approximation of the bubble profile on a two dimensional plane. Though this may seem to be very simple for regular solid projections, things tend to become complicated as we observe real case bubble shapes projections. Extrapolation of the boundary is necessary to actually extract the profiles. The magnitude of extrapolation is not high. The final aim is to get a smooth profile. The TSP was found to be the best suited scheme for extraction of bubble boundary profiles. Every digital image obtained consists of minute square cell areas called pixels. Due to the square shape of the pixels further magnification of the images show irregular boundaries. Hence it is necessary that smoothening of the profile be done. This is the first phase of profile extraction. A profile here means the pixel co-ordinates of the contour extracted from the bubble images.

Solutions to the Traveling Salesman Problem

The traveling salesman problem can be solved using different approaches. A famous approach is the 'brute force' algorithm that would try out all the options of tours, before a favorable solution was agreed upon. In such a case, the net would first determine the number of cities that the salesman would visit. Then a wild guess would be made and a possible route between the cities would be proposed. Two important solution techniques have been described in the following sections.

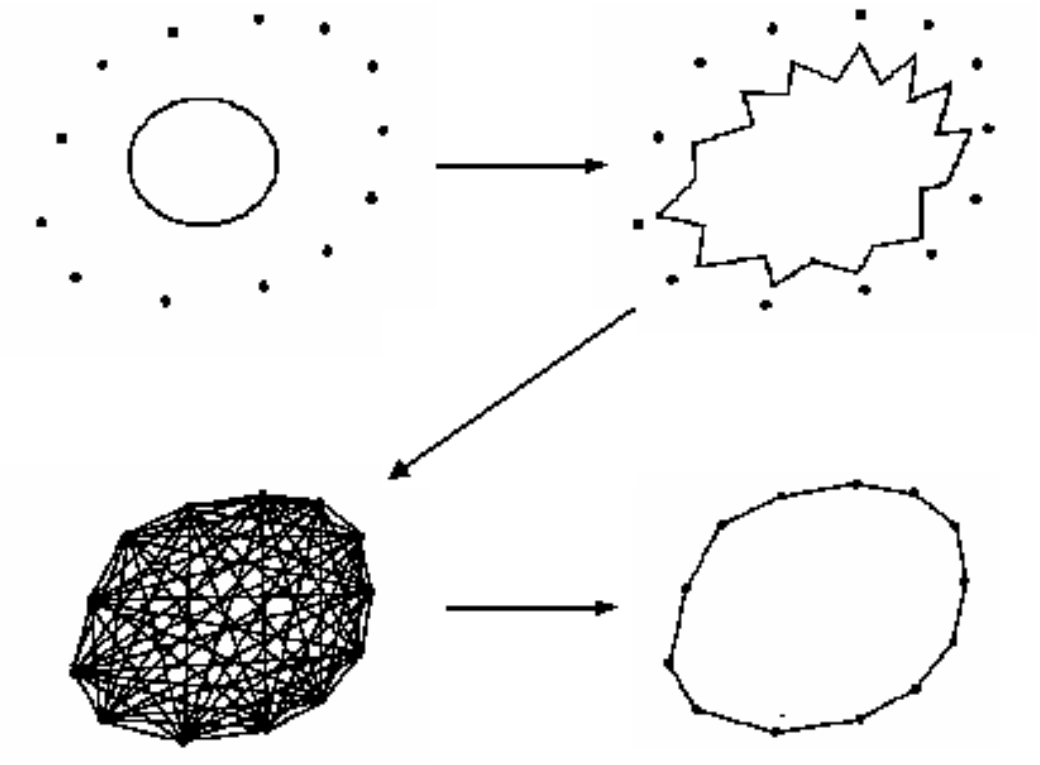

Fig.11. Stages of TSP (Cities are represented as points)

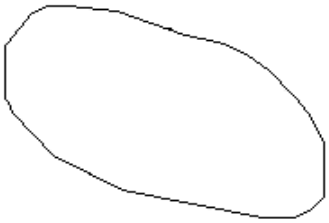

Fig.12. Raw Profile Output from the TSP – SA for the Bubble Shown in Fig.8.

Self Organizing Map Approach

Apart form the SOM approach, the Self Organizing Map [17, 18, 19] approach was also employed to solve the TSP. In this approach, the net is allowed to organize it self and present continuous patterns of the route/ tour till stability is reached. The Eulerian distance between the cities in the proposed route/tour would be estimated in each pattern. A Neural Network based on the Self Organizing Map concept applies the error function minimization technique to achieve minimum error. The error function chosen in such a net is normally the distance between the cities. The net tries would try to optimize the distance between the cities by shortening the distance and changing the route constantly till the error is minimized. A two group neural network based on the 'Self Organizing Maps' was built and tested for use in this technique. Fig.11 shows a graphical illustration of the SOM technique. Fig.12 shows a completed profile of an arbitrary shape using the SOM approach to solve the TSP.

Simulated Annealing Technique

Another well-known algorithm known as the 'Simulated annealing technique' (SA) was also employed and tested to solve the traveling salesman problem. The SA evolved from the principle of the annealing of Spin Glass. The process of cooling metals at a slow and controlled rate is referred to as 'Annealing'. Slow cooling makes the atoms to form a regular crystalline lattice, making the metal less brittle. In forming a regular lattice, it also obtains the 'least' energy state. In effect the lattice is the optimum structure that the particular solid would have attained in order to be in the lowest energy level state. The

SA technique approach can be thought of being comprised of an objective function, an acceptance function, a generating function and the cooling schedule. The objective and the acceptance functions are considered to be the main. The objective function is a mapping transform, which maps the input vector into a scalar. This basically is the function that has to be optimized. The generating function generates the new points among the available data. The acceptance function decides if the point selected should be accepted or rejected. The mathematical representation of the objective and the acceptance functions are as follows.

$$E = f(k) \quad (1)$$

$$g(dE, t) = 1/(1+\exp\{dE/at\}) \quad (2)$$

where, f is the objective function, g is the acceptance function, E is the energy, dE is the change in energy, t is the temperature and c is a weight parameter depending on the type of solid. The Annealing Schedule determines how fast the 'T' goes from a higher value to a lower value.

Further the SA technique as applied to solving the TSP can be divided into three important steps. These are Inversion, Translation and Switching. The Inversion step removes the two vertices from the tour and replaces them in the reverse order. The next step of Translation replaces a section of the tour between two randomly selected consecutive cities. The final switching step selects two cities randomly and switches them in a tour. However the goal of the SA algorithm is to minimize this objective function. In other words, find 'k' (1) such that 'E' (1) is a minimum at 'k'. A code was developed in

MATLAB to solve the TSP using the SA technique choosing the eulerian distance as the optimization function and extract the profile of the bubbles.

Table.2. Comparison of SOM and SA Methods

Number of co-ordinates (cities) on the Contour	SOM- TSP (Min)	SA – TSP (Min)
10	1 to 4	<1
50	> 10	<2
100	NA	<4
300	NA	<5

Comparison of the SOM and SA Approaches

A comparison was made between the SOM based neural network results and the results SA approach. Table.2 gives a comparison of both approaches and the time taken by them to solve the TSP, simulated using a Pentium III machine, for various numbers of cities chosen on a synthetic map. The simulated annealing technique solved the problem in significantly lesser time than the SOM based neural network algorithm. It was observed that as the number of cities increased, the efficiency of the Solution increased, whereas the time taken to arrive at a solution also increased considerably. Though the SA approach was also found to be slow, considering the amount of bubble profiles one had to handle, it was nonetheless, usable for more number of cities (coordinates) with high efficiency. In the present problem the bubble boundaries are quite prominent and hence

the number of co-ordinates that would be available on the contour is huge. Hence the SA approach was employed to solve the TSP considering the obvious advantage of reduced time of analysis and higher efficiency.

CHAPTER VII

BUBBLE SEPARATION TECHNIQUE

One of the toughest problems faced in profile extraction and reconstruction is the occurrence of overlapping bubbles. The possibility of occurrence of overlap in planar views is high. Overlap causes bubbles closer to the cameras to cover completely or partially other bubbles that are away, leading to ambiguities about the shape of the hidden bubble. In such a case one view of the bubble may not be seen at all. Such cases are beyond control owing to the limitations of the image acquisition systems. In some cases, bubbles overlap in the two-dimensional planar view. Hence it is very difficult to predict the profile of these bubbles for the part that is not visible and that are hidden by other bubbles closer to the camera. Two unique methods were developed to solve this problem of overlapping bubbles based on two assumptions as explained in the following sub-sections.

The Conic Assumption

A simple solution to the above mentioned limitation would be to assume that the invisible part of the bubble is of some known shape[5]. This method is illustrated in Fig.13**.** The easiest assumption that one can make is that the hidden profile matches a simple curve normally a Conic section. This reduces the computational time and increases the overall efficiency of the technique. This method was widely used in combination with the method described later in this chapter.

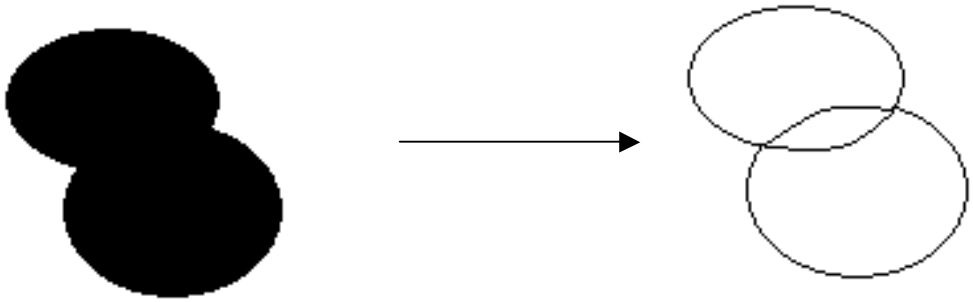

a. Overlapping Bubbles in Shadow Images

b. Bubble Separation Assuming Conic Profiles

Fig.13. Illustration of the Conic Assumption Method

The Zero Curl Assumption

A more complex method would be to observe the bubble shape in the next image pair assuming that it moves with a different velocity as the one that was hiding it. This is normally the case as the bubble shapes vary and so does their velocities. The method is illustrated in the Fig.14. Of course this approach is valid if and only if we assume that in the very short amount of time between (t2-t1) the consecutive pair images, the bubble rotation (Curl) is negligible. If the velocity of the flow is not too large, this assumption may be valid and thus it is possible to reconstruct the bubble profile completely by observing the profile of the same bubble in the next pair of consecutive images. But there is always a huge uncertainty that is associated with such an assumption. During pair transition, (time between the consecutive images pairs) collision of the bubble under observation with other bubbles makes this assumption invalid as it is very hard to even recognize the bubble under observation in the next consecutive pair of images. Hence

accurate separation depends on the degree of uncertainty that one can agree upon. In the present case both the approaches were applied to achieve the bubble separation on a case by case basis. Fig.15 and Fig.16 show the un-separated (raw TSP output) and separated profiles of a large number of bubbles after applying both the techniques.

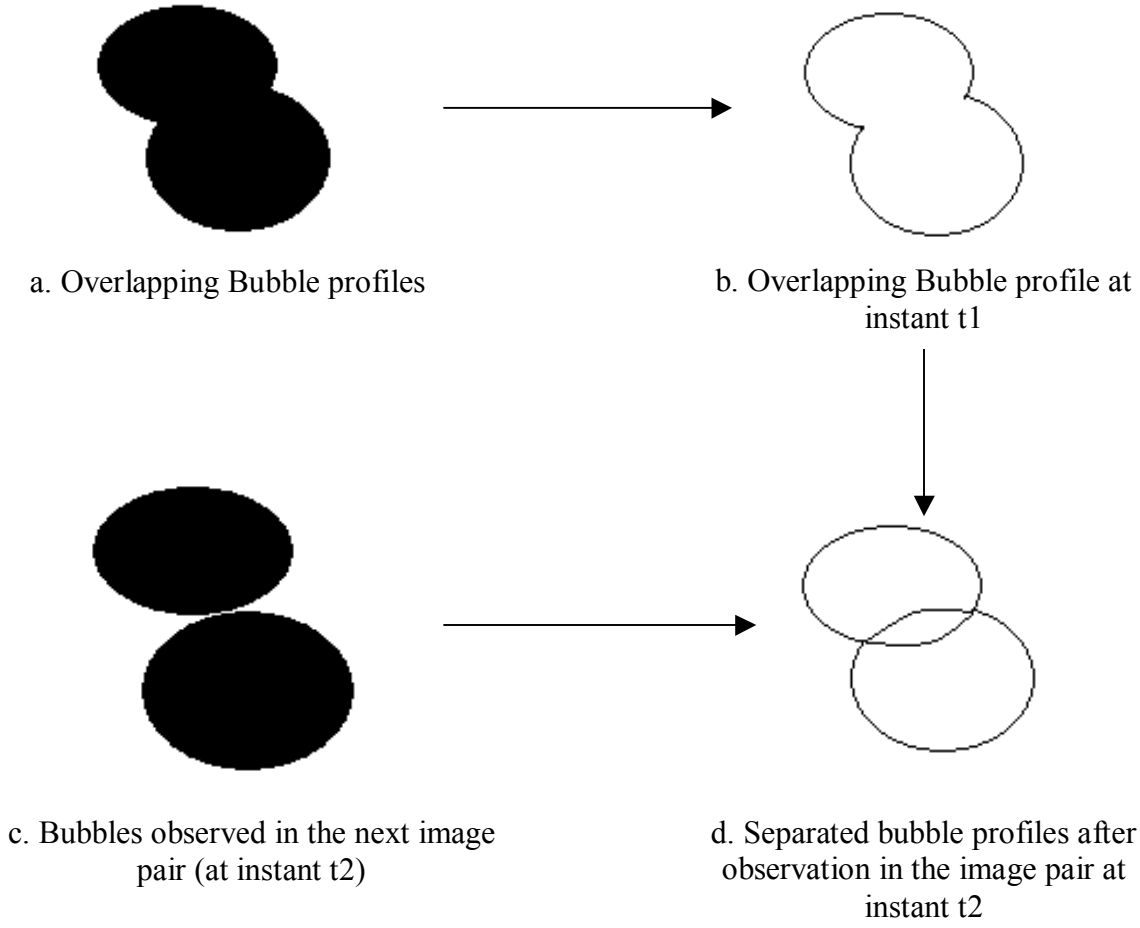

a. Overlapping Bubble profiles

b. Overlapping Bubble profile at instant t1

c. Bubbles observed in the next image pair (at instant t2)

d. Separated bubble profiles after observation in the image pair at instant t2

Fig.14. Illustration of the Zero Curl Assumption Method

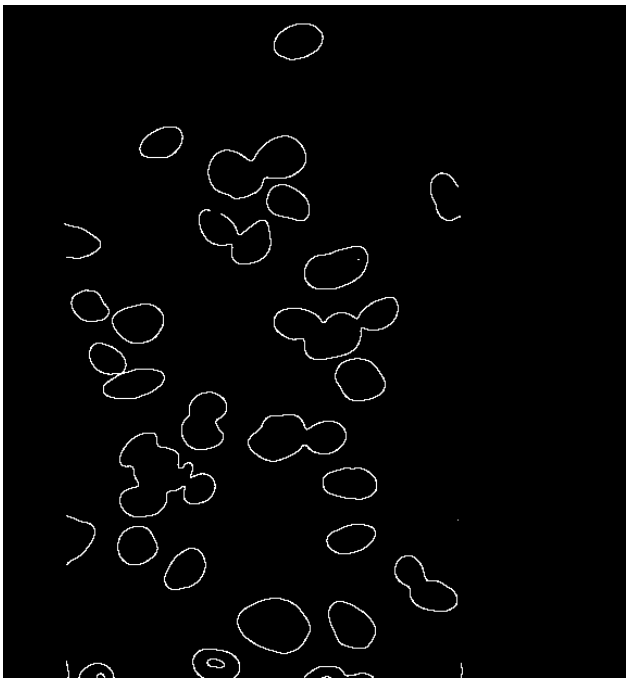

Fig.15. Un-Separated Bubble Profiles

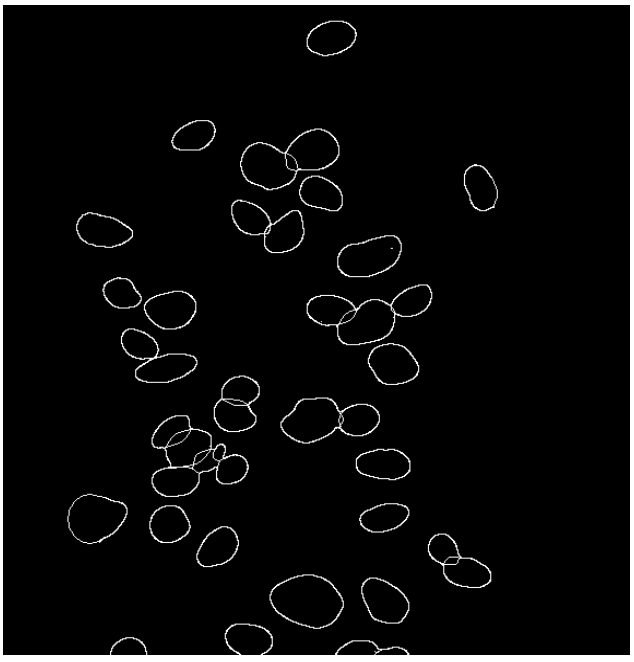

Fig.16. Separated Bubble Profiles Using both Methods

CHAPTER VIII

PROFILE REFINEMENT

As discussed in earlier chapters, the input to the NURBS CAD software is the profile of the bubble. The output of the TSP is just the contour connecting the co-ordinate points located on the bubble boundary. This does not necessarily mean that the output can be used directly. It is often observed that the output profile is highly crude, rough and sometimes discontinuous. In other words, upon careful examination of the digital images, bubble boundaries are not distinct. If we were to join the points on the bubble boundary, such a profile would look 'stepped' or sometimes discontinuous even. This may be the result of possible non-uniform reflection on the bubble surface that causes non-uniformity in the illumination intensity, which passed undetected in the previous stages. This is the characteristic of digital image. Fig.10 of chapter V shows a bubble data input to the TSP- SA algorithm. The output of the TSP-SA is shown in Fig.11 of chapter VI. It is observed that the bubble profile is highly rough and stepped. Though NURBS, which is considered to be a highly flexible tool for reconstruction and can be modified to take into account the roughness, in reality bubble surfaces are not found to have such high degree of roughness. Hence the profile has to be smoothened. This amounts to reducing the number of cities needed for analysis. A technique was applied to select the optimum number of cities, form the group of cities that were detected during thresholding and Preliminary TSP-SA solution.

The bubble raw profile was divided into two parts, the left and the right. The topmost and the bottom most pixels on the boundary were chosen as the end points of the line cutting the profile into the left and the right parts. In the pixel intensity matrix of the left half of the profile, the left most pixels of each of the rows were retained. Similarly the right most pixels were retained in the right half of the profile. This in effect lessened the number of cities, decreasing the required analysis time and eliminated the ambiguity to a certain extent in determining the number of cities that had to be taken into analysis. The data was again fed to the TSP-SA code. The output was a smooth profile of the bubble. Fig.17c shows the smooth profile after refinement technique was applied to the profile shown in Fig.17b.

a. Shadow Image

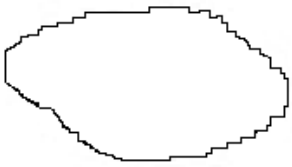

b. Raw Profile

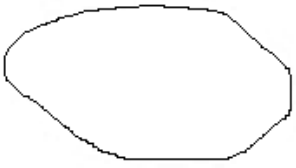

c. Smooth Profile

Fig.17. Profile Refinement Technique

CHAPTER IX

THREE DIMENSIONAL RECONSTRUCTION

This chapter discusses the final step of the reconstruction technique. The discussion pertains to the tools used for reconstruction, the reconstruction interface, the three dimensional reconstruction procedure and results for a single isolated bubble and a batch of thirty bubbles selected from a shadow image.

Non Uniform Rational B Splines

NURBS as they are commonly known, are standard tools used in industry for deign and geometry representations. NURBS are general combinations of non-rational B-Splines, and Bezier curves and surfaces [16, 39]. They normally offer a single mathematical basis on which standard mesh shapes and standard analytical shapes [16] are represented. The NURBS representation offers a greater flexibility when it comes to modeling free form geometries, especially in perspective transformations. The NURBS method can be implemented using robust and accurate algorithms.

Computer Aided Design and Reconstruction Interface

After the two orthogonal, one-dimensional profile was extracted using the TSP – SA techniques, and the refinement had been made, the data was imported into a RHINO-NURBS CAD reconstruction program. An evaluation version of the Rhinoceros – NURBS Modeling CAD program used was for the reconstruction purposes. The CAD

was found to be the most flexible and agreed with industrial standards for design. NURBS (Non-Uniform Rational B-Splines) is a typical parametric solid modeling scheme with scope for accounting the free form of objects of highly irregular shape structures and deformations. The profiles were imported into the CAD worksheet for further reconstruction with their co-ordinates preserved as in the original image. I other words, care was taken that the coordinates of CAD and the images matched one to one.

Profile and Centroid Matching

It is very important to know the centroid of the bubbles in order to track them. This is also important for reconstruction. This is necessary as only by observing the projection of the three-dimensional object on to a plane perpendicular to the view, the three-dimensional orientation, especially the 'back tilt', of any object with respect to the vertical axis cannot be estimated. It follows from solid geometry that the centroids of both the images align if only if the orientations are proper. After the profiles are imported into the CAD program, they were placed orthogonal to each other and the centroids of each of the one-dimensional area contours were estimated. The only information that is common to both the orthogonal profiles is the maximum and minimum points on the bubble boundaries. Keeping the maximum and minimum points and the area centroids unchanged, the profiles were iteratively rotated around the area centroids and scaled till the profiles exactly matched. A constant visual observation was made to check these actions of three-dimensional rotations and ensure that they did not make the projections

of the reconstructions out of match with the actual two views of which we already had enough information.

Three Dimensional Reconstruction

Using the advanced tools like Rail Revolve[20] with the scale option and surface matching available for surface reconstruction with the chosen RHINO CAD software, the bubble three-dimensional surface profiles were reconstructed. The results of such a reconstruction are shown in the Fig.18. The advantage is that at a time eight views of the bubbles can be recorded.

Bubble Placement

The one to one correspondence discussed in the previous chapters, was maintained throughout the process and hence, eliminated the ambiguity of bubble locations. However the distances of the bubbles in both the views, from the walls, were measured and verified with that of the actual images.

Results of Reconstruction

An image pair for low Reynolds number (3000) flow, consisting of about 34 bubbles was reconstructed and the three dimensional results are shown in Fig.19b. Fig.19a shows sample SIV images used to extract the bubble profiles for reconstruction.

a. Front View

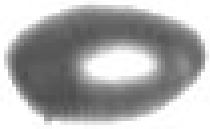

b. Side View

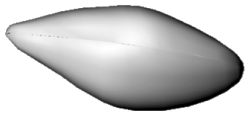

c. Reconstructed Front View

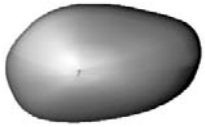

d. Reconstructed Side View

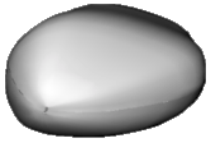

e. 3D Profile of a Reconstructed Bubble

Fig.18. Reconstruction of a Single Separated Bubble

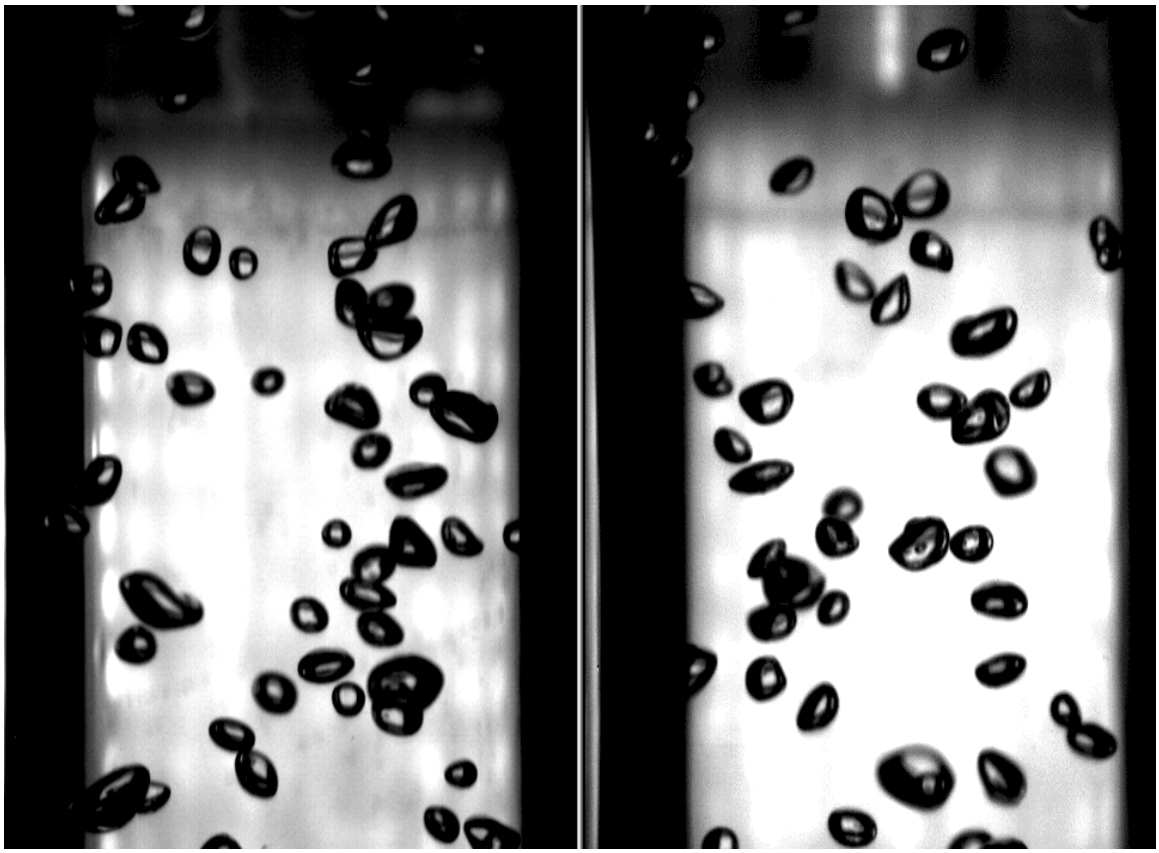

Fig.19a. Orthogonal Shadow Image Views

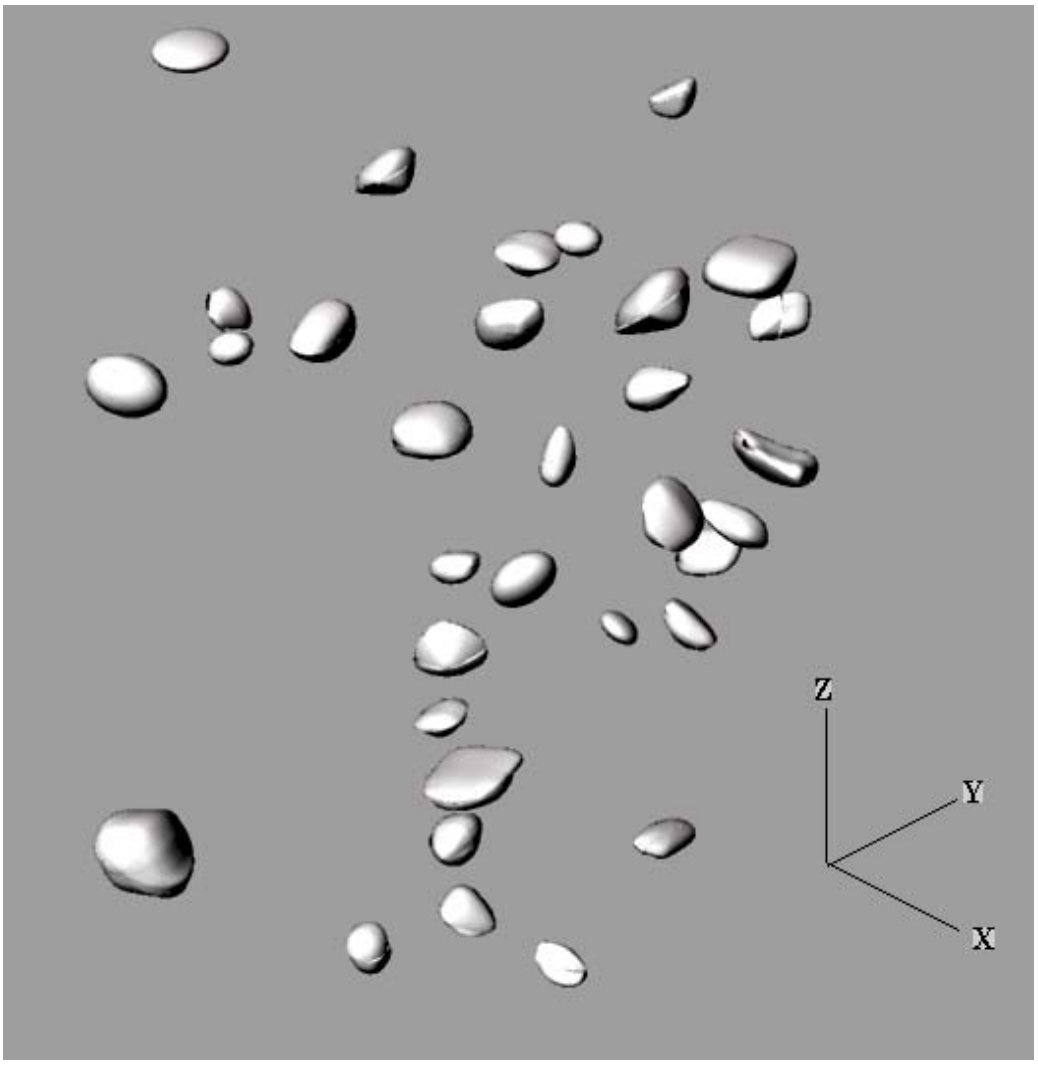

Fig.19b. 3-D View of Reconstructed Bubbles Using Two Orthogonal, Two Dimensional Boundary Profiles

CHAPTER X

APPLICATIONS OF THE TECHNIQUE

A brief study was made regarding the applicability of the technique to two important sections. The technique was used to estimate the void fractions of the mixture and at a particular depth of the pipe. Secondly, the technique was applied to track bubble trajectories in the flow field and calculate the bubble velocities.

Void Fraction

Void Fraction is an important parameter in two phase flows. It is defined as the ratio of volume of the discrete phase to the total volume (both discrete and continuous). The void fraction at a particular depth of the channel is defined as the ratio of the area of the discrete phase to total area. The void fraction at a particular depth can hence be estimated if the area of both the liquid and the air/gas present are known.

Void Fraction of the Mixture

The reconstruction facilitates the estimation of the volume and surface area of the bubbles using suitable CAD (*Rhino 3.0*) commands. The estimated volume of the bubble is used to calculate the bulk void fraction of the mixture. The bulk void fraction is calculated using equation (3)

$$\alpha = \frac{\text{(Volume of all the bubbles in an image)}}{\text{(Volume of the section under investigation)}} \qquad (3)$$

Void Fraction at a Particular Depth

This technique was further extended to estimate the void fraction at a particular depth of the channel/pipe. Advanced CAD tools facilitate the sectioning or splitting of the bubbles at a particular depth. These sections can then be projected as seen from the top view. The area of this projection can be calculated using the tools available from the CAD software. The void fraction at that particular depth is calculated using equation (4).

$$\alpha = \frac{\text{Area of the projection}}{\text{Area under investigation}} \qquad (4)$$

This technique is illustrated using a single bubble. Fig.20a shows the front-view of a reconstructed profile. Fig.20b shows the bubble after it is split at a specified depth. Fig.20c shows the top view of the same bubble. The depth, at which the void fraction is to be estimated, is indicated by the cutting plane xx, as shown in Fig 20a. Fig.20d shows the three-dimensional split of the bubble along the cutting plane. Fig.20e shows planar projection of the split part in three dimensions. Fig.20f. shows the projection of the spilt surfaces on the plan, which is the horizontal plane.

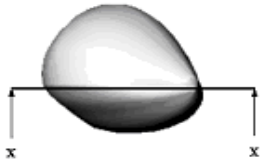

a. Front View of the Reconstructed Bubble, xx indicates, the Cutting Plane

b. Bubble after the 'Split'

c. Top View of the Bubble

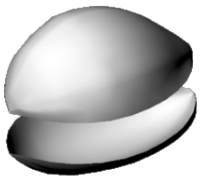

d. Three-Dimensional View after the Split

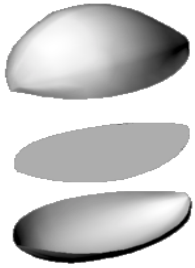

e. Projection of the Split Surfaces Shown in 3D

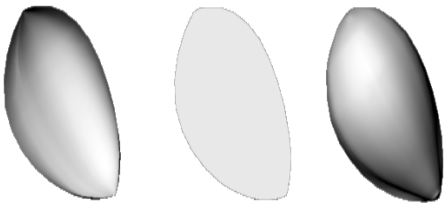

f. Projection of the Surfaces on the Plan Shown in Top View

Fig.20. Calculation of the Void Fraction at a Particular Depth

Bubble Trajectory Tracking

As mentioned in the earlier sections, with the improvement in three dimensional visualization techniques, it has become a necessity to include bubble trajectories on the flow field vector mappings. Reconstruction and availability of the centroid facilitates the lagrangian tracking of the bubble along its path. A simple tracking program[40] developed in MATLAB was used to track a single bubble along its path and the resultant velocity vector vectors were estimated. The results are shown in Fig.21a and Fig.21b. The velocity of the bubble can be estimated knowing the relative locations of the volume centroids of the reconstructed bubbles from consecutive images. Knowing the time between the PSIV pulses, the three dimensional bubble velocity (Vb) can be calculated using equation 5.

$$Vb = (\{(x2-x1)^2 + (y2-y1)^2 + (z2-z1)^2\}^{0.5}) / (\text{Time between Laser pulses}) \quad (5)$$

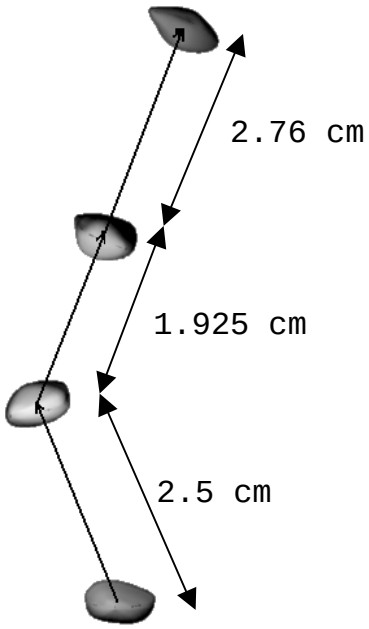

a. Path of the Bubble as seen in Front view

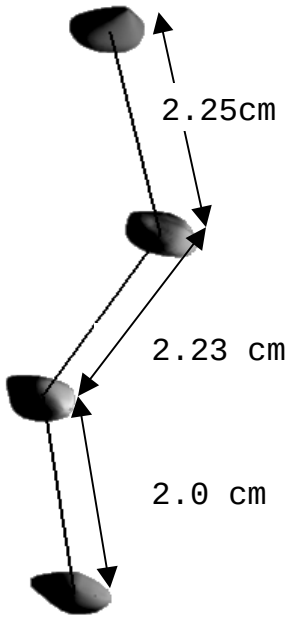

b. Path of the Bubble as seen in Side view

Fig.21. Bubble Trajectory Tracking (High Reynolds Number Flow)

CHAPTER XI

LIMITATIONS OF THE TECHNIQUE

The technique inherently does suffer from certain limitations. As such the limitations are not pertaining to the procedure of the technique but the hardware associated with data acquisition.

The first of such limitations was recognized to be the number of views of the bubbles that was available. It should be noted that it is practically impossible to cover the whole three dimensional profile of the object visually. It was found that two views were sufficient to reconstruct the bubbles quite accurately as the bubbles were not found to be highly irregular in shape. The curvatures were found to be often smooth and continuous sufficing three dimensional reconstruction needs with just two orthogonal views.

The second limitation was the non-distinct boundary of the bubbles in the images. Though this was effectively handled during the thresholding stages, the loss of data especially near to the bubble edge was inherent. This also was found to affect the 'yield' in the number of co-ordinate points on the bubble boundary (cities) used for reconstruction, which were extracted using different threshold limits The demarcation of the bubble boundary is extremely difficult with the varying intensity of illumination and reflection at the bubble surface. Fig.22 shows the plot of the surface area versus different threshold levels (normalized) for a single bubble using the Grade C method discussed in the earlier chapters.

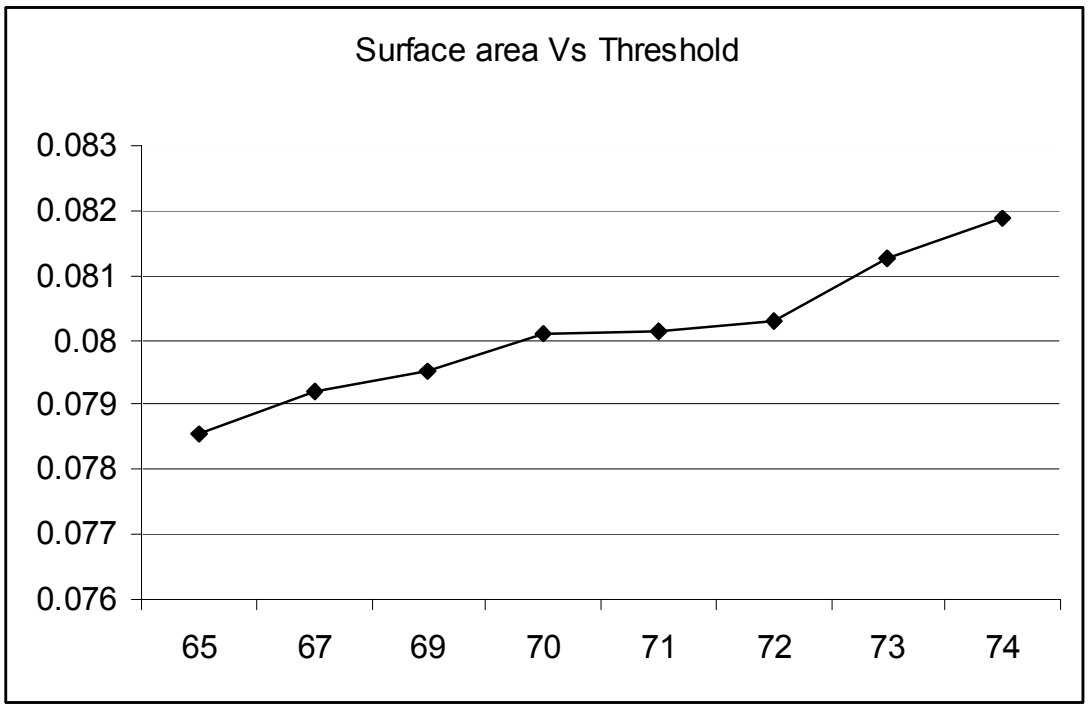

Fig.22. Plot of Surface Area vs. Threshold Limit

The third limitation was the case of the overlapping bubbles. Though two techniques described in chapter VII were employed, the Zero Curl method often failed to separate overlapping bubbles in high speed flows with large bubble densities. The fact that the zero curl method failed was due to two main system limitations. The first being collision of the bubble under investigation with other bubbles which often caused serious shape deformations, rendering it impossible to recognize the same bubble in the next image. The second limitation was due to other bubbles moving in the visual plane covering the bubble under investigation. This limitation necessitated the use of the ellipse assumption method in cases where the zero curl method failed. This was a sort of trade off between accuracy and possibility of three dimensional reconstructions.

CHAPTER XII

CONCLUSION & RECOMMENDATIONS

An attempt has been made to propose a new integrated method for reconstruction of bubbles in fluid flow, in contrast to the original ellipsoidal reconstructions and the results were found to be satisfactory. Though limitations in some steps of the technique seem prominent, useful and acceptable approximations have been proposed to overcome the limitations. I trust that further development in this path and regard shall prove beneficial in understanding the behavior of bubbles in a flow to a larger extent.

This technique demonstrates the capability and applicability of NURBS modeling and neural network approaches as applicable to fluid flow problems in particular and three-dimensional reconstruction in general. Using the well know combinatorial optimization problem in extraction of the bubble profiles has been successfully observed and applied for bubble profile extraction and reconstruction for the first time.

The application of the technique in calculating the void fraction and tracking the bubbles has been demonstrated. Further it is believed that one can extend this technique to develop models to observe bubble reconstruction and growth. Further, this technique can be combined with three-dimensional PIV to study the behavior of the gas-liquid mixture.

REFERENCES

1. ADRIAN .R.J, "Particle-Imaging Techniques for Experimental Fluid Mechanics", *Annual Review of Fluid Mechanics*, **23**, 261 (January 1991).

2. T. KURIHARA, H. CHOI and G. MATSUI, "Measurement of Velocity Field and a Particle/Bubble Motion by PIV and PTV", *9th. International Symposium on Flow Visualization*, Edinburgh, Scotland (August 2000).

3. E. A. COWEN and S. G. MONISMITH, "A Hybrid Particle Tracking Velocimetry Technique", *Experiments in Fluids*, **22**, 199(1997).

4. O. V. JAVIER, "Three-dimensional Experimental Investigation of the Shape and Dynamics of a Rising Bubble in Stagnant Water with Particle Tracking Velocimetry", Ph.D. Dissertation, Texas A&M University, College Station, TX. (1999).

5. R. DONALD TODD, **"**Methodologies for Analyzing PIV and SIV Results from a Two-Phase Air/Water Experiment", Ph. D. Dissertation, Texas A&M University, College Station, TX, (December 2002).

6. P. CENEDESE, ROMANO, PAGLIALUNGA and TERLIZZI, "Neural Net for Trajectory Recognition in a Flow", *6th International Symposium on Applications of Laser Techniques to Fluid Mechanics*, Lisbon (July 1992).

7. G. LABONTE, "A SOM Neural Network That Reveals Continuous Displacement Fields", *Proc of the 1998 International Joint Conference on Neural Networks at WCCI '98* , Anchorage(June 1998).

8. Y. HASSAN and O. PHILIP, “A new Artificial Neural Network Tracking Technique for Particle Image Velocimetry”, *Experiments in Fluids*, **22** (1997).

9. M. HASSOUN, *Fundamentals of Artificial Neural Networks*, the MIT Press, Cambridge (1995).

10. S. LIN, "Computer Solutions of the TSP", *Bell Systems Technical Journal*, **44**, 2245 (1965).

11. Traveling salesman homepage, *http://www.math.princeton.edu/tsp* (2002)

12. C. SKISCIM and B. GOLDEN, “Optimization by Simulated Annealing - A Preliminary Computational Study for the TSP”, *Proceedings of the 15th Conference on Simulation*, **2**, 523 (October 1983).

13. M. JUNGER, G. REINELT, S. THIENEL, “Provably Good Solutions for the Traveling Salesman Problem”, IWR, Heidelberg (1994).

14. H.HAROLD SZU and RALPH HARTLEY, “Fast Simulated Annealing”, *Physics Letters A*, **22**, 157(1987).

15. B. ZHANG and A. PANG, “NURBS Blobs for Flow Visualization”, A Technical Report, UCSC (2000).

16. JAMES D. FOLEY, *Introduction to Computer Graphics*, Addision-Wesley, New York (1994).

17. T. KOHONEN, “Analysis of Self Organizing Process”, *Biological Cybernetics*, **44**, 135 (1982b).

18. T. KOHONEN, “Self Organizing Maps: Optimization Approaches”, *Artificial Neural Networks*, **2**, 981 (1991).

19. T. KOHONEN, "Self Organized Formation of Topologically Correct Feature Maps", *Biological Cybernetics*, **43**, 59 (1982a).

20. RHINO 3.0, Rhinoceros, NURBS modeling for Windows, *www.rhino3d.com*. (2002)

21. S. HILGERS, W. MERZKIRCH and T. WAGNER, "PIV Measurements in Multiphase Flow using CCD and Photo-camera", *ASME FED* **209,** 151 (1995).

22. K.NISHINO, N. KASAGI and M. HIRATA, "Three-dimensional Particle Tracking Velocimetry Based on Automated Digital Image Processing" *Trans. ASME J. Fluids Eng.* **111,** 384 (1989).

23. K.MIYAZAKI, G.CHEN, F.YAMAMOTO and K.HORII "Gas-Solid Two-Phase Spiral Flow Investigation with PIV Techniques", *Transactions of the Japan Society for Aeronautical and Space Sciences*,**41**, p.163 (1999).

24. X.TU and C.TRÄGÅRDH, "Methodology Development for the Analysis of Velocity Particle Image Velocimetry Images of Turbulent, Bubbly Gas-Liquid Flows", *Measurement Science and Technology*, **13**, 1079, (July 2002).

25. H.M.CHOI, T.KURIHARA, H.MONJI and G.MATSUI, "Measurement of Particle/Bubble Motion and Turbulence Around it by Hybrid PIV", *Proc. of Second Japanese-European Two-Phase Flow Group Meeting,* Tsukuba, Japan (September 2000).

26. A. FUJIWARA, A.TOKUHIRO and K. HISHIDA, "Application of PIV /LIF and Shadow Images to a Bubble Rising in a Linear Shear Flow", *10th International Symposium on Applications of Laser Techniques to Fluid Mechanics*, Lisbon (July 2000).

27. G. MATSUI, H. M. CHOI, H. MONJI and T. TERAUCHI, "Hybrid PIV Combined with 3D-PTV for Particle-Fluid Interaction", *Proc. of The 3rd International Symposium on Measurement Techniques for Multiphase Flows*, Fukui, Japan, p.180 (2001).

28. T.KAWAGUCHI, T.KOBAYASHI, K.HISHIDA and M.MAEDA, "Measurement of Small Droplet- and Bubble-Sizing by an Improved Interferometric Laser Imaging (ILIDS) Technique," *Proc. Of The 3rd International Symposium on Measurement Techniques for Multiphase Flows* (2001).

29. H.G. MAAS, A. GRUEN and D. PAPANTONIOU, "Particle Tracking in three-dimensional turbulent flows - Part I: Photogrammetric Determination of particle Co-ordinates", *Experiments in Fluids*, **15**, 133 (1993).

30. K.OHMI, "New Algorithms in Particle Tracking Velocimetry", *Image Processing Methods in Applied Mechanics* (May 1999).

31. K. S. OBERMAYER, "A new Particle Tracking Algorithm on Deterministic annealing and alternative distance measures", *Experiments in Fluids* (1999).

32. Y. HASSAN. D. S. WILLIAM and J. O. VILLAFUERTE, "Three Dimensional Bubbly Flow Measurements using PIV", *Journal of Flow Visualization*, **1**, January 1999.

33. D. A. TURNER, I. J. ANDERSON and J.C. MASON, "An Algorithm for fitting an ellipsoid to data", National Physical Laboratory, UK, 1999.

34. A.B. FORBES, "Fitting an Ellipse to data", Technical Report DITC 95/87, National Physical Laboratory, UK (1987).

35. E. DAVIES, "Theory, Algorithms and Practicalities", *Machine Vision*, Academic Press, Chap. 4.

36. R. GONZALEZ and R. WOODS, *Digital Image Processing*, Addison-Wesley Publishing Company, Chap. 7. (1992 ed).

37. D. VERNON, *Machine Vision*, Prentice-Hall, p.49, p.86 (1991).

38. F.YAMAMOTO, M. IGUCHI, J. OHTA and M. KOKETSU, "Measurement of Bubbling Two Phase Flow using 3-D PTV based on Binary Image Cross Correlation Method", FED -Vol 209, Flow Visualization and Image Processing of Multiphase Flow Systems, *Proceedings of the 1995 ASME/JSME Fluids Engineering and Laser Anemometry Conference and Exhibition*, Hilton Head, South Carolina, p.131 (August 1995).

39. M. BRILL, H. HAGEN, H. C. RODRIAN, W. DJATSCHIN and V. K. STANISLAV, "Streamball Techniques for Visualization*", Proc. of Visualization*, Washington D.C., p. 255 ACM (October 1994).

40. D.P. HART, "Super Resolution PIV through Recursive Local Correlation", *VSJ-SPIE International Conference on Optical Technology and Image processing in Fluid, Thermal and Combustion flow*, Yokohoma, Japan (December1998).

Other Sources Consulted

L. CHEN and AIHARA, "Chaotic Simulated Annealing by Neural Network Model with Transient Chaos", *Neural Networks*, **8**, 915 (1995).

W. J. CONOVER, *Practical Nonparametric Statistics*, John Wiley and Sons, New York (1980).

F. DAVID ROGERS and J. ALAN ADAMS, *Mathematical Elements of Computer Graphics (2nd ed.)*, McGraw-Hill, New York (1990).

D. P. HART, "PIV Error Correction", *Experiments in Fluids*, **29**, 13 (1999).

M. JUNGER and D. NADDEF (editors), "TSP Cuts Which do not Conform to the Template Paradigm", *J.* of *Computational Combinatorial Optimization*, **7**, p.261 (2001).

S. KIRKPATRICK, C. D. GELATT. JR and M. P. VECCHI, "Optimization by Simulated Annealing", *Science*, **11**, Number 4598, p.671 (May 1983).

S. KIRKPATRICK, C. D. GELATT, and M. P. VECCHI, "Optimization by Simulated Annealing", *IBM Computer Science/Engineering Technology Report*, IBM Thomas J. Watson Research Center, Yorktown Heights, New York (1982).

T. KOHONEN, "A Simple Paradigm for Self Organized Formation of Structured Feature Maps", *Lecture Notes in Biomathematics 45 - Competition and Co-operation in Neural Nets*, Springer-Verlag, New York (1982).

P. KROLAK, W. FELTS and G. MARBLE, "A Man-Machine Approach Towards Solving the Traveling Salesman Problem", *Communications of the ACM*, **14**, 327 (May 1971).

N. METROPOLIS, A. ROSENBLUTH, M. ROSENBLUTH, A. TELLER, AND E. TELLER, "Equation of State Calculations by Fast Computing Machines", *J. of Chemical Physics*, **21**, 1087 (1953).

R. G. MICHAEL, S. J. DAVID*, Computers and Intractability: A Guide to the Theory of NP-Completeness*, W. H. Freeman & Co., New York (1979).

E. M. MORTENSON, *Geometric Modeling*, John Wiley and Sons, New York (1985).

J. P. NORBACK and R. P. LOVE, "Geometric Approaches to Solving the Traveling Salesman Problem", *Management Science*, **23**, 1208 (1977).

H.G PAGENDARM and F.H.POST "Studies in Comparative Visualization of Flow Features" *IEEE Computer Society's Seminar on Scientific Visualization*, Dagstuhl, Germany, **4**, 211 (May 1994).

W. R. STEWART, "A Computational Comparison of Five Heuristic Algorithms for the Euclidean Traveling Salesman Problem", *Evaluating Mathematical Programming Techniques*, (Ed., John Mulvey), Springer-Verlag, New York (1982).

W. R. STEWART, "A Computationally Efficient Heuristic for the Traveling Salesman Problem", *Proceedings of the 13th Annual Meeting of Southeastern TIM S*, Myrtle Beach, S.C., p.75 (1977).

E. WASIL, B. GOLDEN and A. ASSAD, "Alternative Methods for Comparing Heuristic Procedures on the Basis of Accuracy", University of Maryland, Management Science and Statistics Working Paper #MS/S 83-012 (1983).

F.M. WHITE, *Fluid Mechanics (3rd ed.)*, McGraw-Hill, New York (1994).

S. YOSHIDA, "Trajectories of Rising Bubbles", *Proc. Of the 16th Japanese Multiphase Flow Symposium, Touya, Hokkaido* **(**July 1997).

H. YUAN, H.N. OGUZ AND A. PROSPERETTI, "Growth and Collapse of a Vapor Bubble in a Small Tube", *International Journal of Heat Transfer*, **42**, 3653 (1999).

VITA

Gokul Vasudevamurthy was born on 19th November, 1977, in Bangalore, India, to Mr. M.S. Vasudevamurthy and Mrs. Leela Kadagathur. He finished his high school and pre-university education at the prestigious National Education Society, Bangalore, India. Later he graduated with a Bachelor of Engineering degree in electrical and electronics engineering with distinction from Bangalore University, India in August 1999. He was associated with the higher mathematics wing of the Department of Science and Technology, Government of India, in the capacity of Student Scholar and Research Assistant Student Fellow between August 1996 and September 2001. He was awarded the merit student scholarship and Junior Research Fellowship, for his work in the field of solid geometry and complex transformations. After his graduation, he worked as an Engineer at SIEMENS Power Engineering (SIEMENS KWU.AG) between August 1999 and October 2000. He joined the Department of Electrical Engineering, Bangalore University, in October 2000 and worked as a lecturer before joining the Department of Nuclear Engineering at Texas A&M University as a graduate student in the August of 2001. He received his Masters Degree in nuclear engineering in December of 2003.